COMPARISON OF A FULLY EMPIRIC AND A SEMI-EMPIRIC NOISE MODELING APPROACH FOR A CARGO-UAV

M. Schmähl, Technical University of Munich, Garching, Germany, 85748
B. Nagy, Technical University of Munich, Garching, Germany, 85748
M. Hornung, Technical University of Munich, Garching, Germany, 85748

Abstract

The two main categories in aircraft noise modeling are fully empiric and semi-empiric approaches. In terms of conventional aircraft noise questions of best practices for noise modeling have been largely clarified. Despite, unmanned aerial vehicle (UAV) systems exhibit a greater variety of mission types and configurations and, thus, UAV noise modeling requires further research. In this work a fully empiric and a semi-empiric noise model of a cargo UAV in horizontal flight are created and compared regarding model accuracy, modeling effort and noise data requirements. The problem of noise fluctuations in turning flight that originate from interaction noise is addressed by introducing bank angle dependent confidence bounds to both models. Subsequently, a discussion of possible noise model applications and an outlook to future noise modeling work of multirotor systems conclude this work.

Keywords

Flight noise modeling, empiric modeling, semi-empiric modeling, system identification

1. MOTIVATION OF UAV NOISE MODELING

In the field of measurement data-based aircraft noise modeling two basic approaches are found: Semi-empiric models include a priori knowledge about sound generation and propagation into a model ansatz which is usually determined by means of system identification. In contrast, fully empiric models are solely data based.

Aircraft noise modeling of conventional aircraft has been intensively researched in the last decades [1] [2] usually focusing on noise emitted during arrival and departure in a vicinity around an airport. Questions of best practices for noise modeling have been largely clarified. Tools based on fully empirical models have a high prediction accuracy for long-term scenarios. Due to this capability such tools are frequently used for application in air-traffic management and legislation processes. Despite, scientific tools that aim to predict single flight events with high accuracy are usually semi-empiric in nature [1, p. 1]. Unmanned aerial vehicle (UAV) systems exhibit a greater variety of mission types and configurations and in urban air mobility (UAM) applications they operate in much smaller distances to urban areas. Thus, optimal approaches to general UAM noise modeling are requiring further research.

In this work a fully empiric as well as a semi-empiric UAV noise model are created based on an identical flight noise measurement data set. The target is to clarify how fully empiric and semi-empiric UAV noise models compare to each other with regards to model accuracy and modeling effort.

2. NOISE MODEL CREATION

2.1. Noise Data Pre-Processing

During project “Raumbezogene Modellierung zur Lärmreduktion elektrischer Senkrechtstarter” (RAUMOLES) inflight noise measurements of the cargo UAV Manta Ray by Phoenix-Wings were conducted, see Figure 1. The narrow band noise data was synchronized with the flight measurement data and the synchronized data set was then used to compute semi-empiric noise models. That work was published in [3] and [4]. Compared to the RAUMOLES data pre-processing, two additional processing steps are added in this work. The effects of atmospheric damping and the Doppler frequency shift are eliminated in the data set. This treatment makes the source noise data independent of the microphone locations and, thus, increases the maximum achievable noise model accuracy.

Figure 1: eVTOL UAV Manta Ray by Phoenix-Wings

2.2. Noise Data Analysis

All noise modeling approaches require model input parameters. Meaningful parameters can be identified through a correlation analysis between UAV states like e.g. propeller speed and the sound pressure level (SPL) recorded by the microphones. Figure 2 displays the result of such a correlation analyses between UAV ground speed *v*, pusher propeller rotation rate *N*, electric power consumption P_{el}, distance between UAV and microphones and measured SPL for the Manta Ray UAV. *N* as well as P_{el} show a similar correlation with SPL. If *N* is chosen as model parameter then the air speed has to be included as a model parameter, too, as the advance ratio and therefore also thrust and noise emission of a propeller at constant rotation rate vary with varying air speed. As the air speed data of the UAV is unavailable and for the sake of simplicity P_{el} is chosen as the only model input parameter in this work.

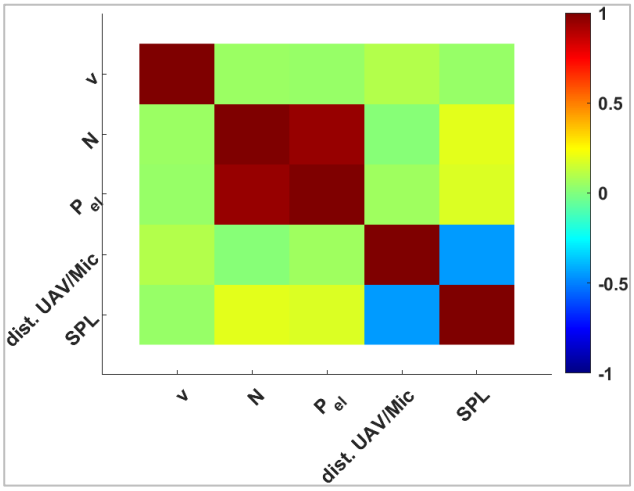

Figure 2: correlation matrix

2.3. Fully Empiric Noise Modeling

The sound prediction of a fully empiric noise model is based on noise emission surface data that represent the SPL at a specific azimuthal and polar noise emission angle relative to the UAV. Such noise emission surfaces exist for a number of discrete model input parameter values. The model is evaluated by, firstly, interpolating the SPL for a distinct emission angle in each noise emission surface and, secondly, by interpolating the final SPL of the model input parameter value under consideration from these SPL values. Finally, the SPL is converted from the reference distance of the noise emission surfaces to the actual UAV observer distance using geometric spreading.
In order to compute these noise emission surfaces for the Manta Ray UAV the synchronized noise data is sorted according P_{el} and three intervals are defined. The P_{el} mean values within these three intervals constitute the model input parameter vector for interpolation between the noise emission surfaces. Finally, the noise emission surfaces are computed based on a modified ridge estimator [5], see Figure 3. The averaged offset between surface 1 and 2 respectively between surface 2 and 3 is 1.0 dB(A) which means that increasing the non-dimensionalized electric power consumption by circa 0.2 increases the noise emission by circa 1.0 dB(A).

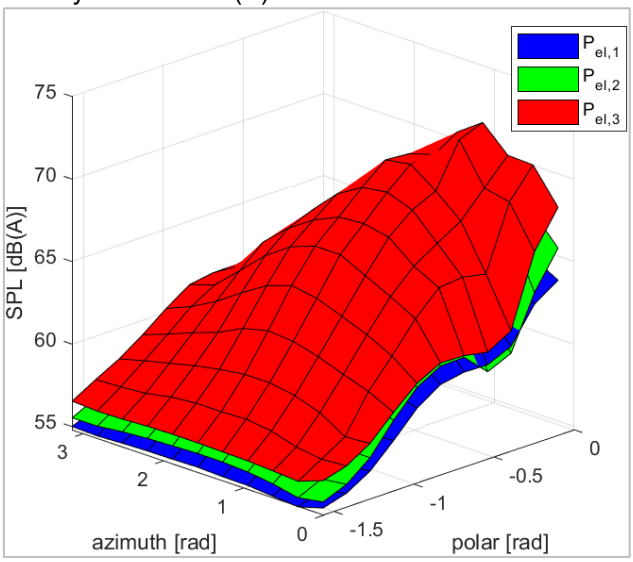

Figure 3: noise emission surfaces at $P_{el,1}$=1.002, $P_{el,2}$=1.179, $P_{el,3}$=1.386; azimuth = 0 rad corresponds to flight direction; polar = -π/2 corresponds to downwards direction; left/right symmetry is assumed

[4] points out the fact that the SPL fluctuations during turning flight are significantly higher than ones during straight flight and assumes that these fluctuations are caused by interaction phenomena. In order to account for this effect bank angle dependent confidence bounds are computed. Figure 4 displays the residual of the noise measurement data and the fully empiric model result over the UAV bank angle as well as the corresponding upper and lower confidence bound. It can be seen that the confidence bounds are most narrow during straight flight where bank angles tend to zero.

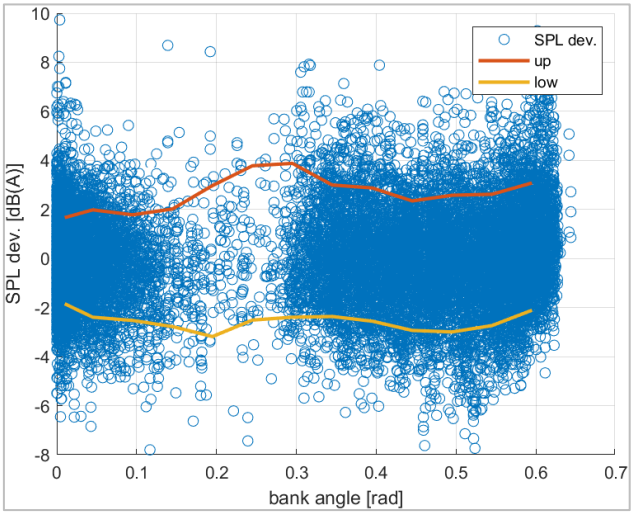

Figure 4: SPL empiric model deviation over bank angle and 80 % confidence bounds

The computation of noise emission surfaces and confidence bounds is repeated for turning flight and for straight flight data in order to compare the accuracy of the model types and model variants in the following chapters in more detail. Figure 5 shows the confidence bound corridor heights of all three model variants (all data, straight flight data only, turning flight data only) which is a direct measure for the model accuracy. It can be seen that the variant using turning flight data exhibits the narrowest corridor heights at bank angles higher than 0.15 rad. This finding demonstrates that splitting the model into a turning flight and into a straight flight model part has the potential to increase the overall noise model accuracy.

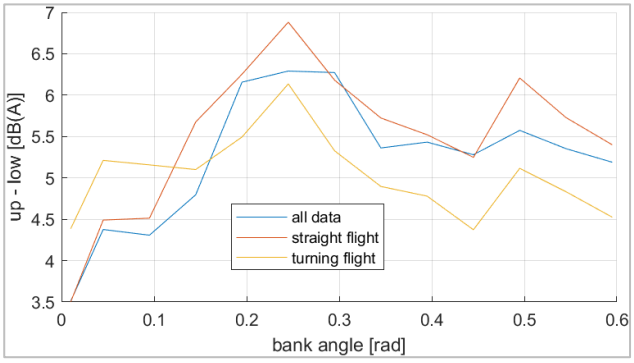

Figure 5: confidence bound corridor height for all three modelings and a confidence of 80 %; corridor height = upper bound – lower bound

2.4. Semi-empiric Noise Modeling

The semi-empiric noise model approach applied in this work was proposed for the first time in [6] and is adapted to the Manta Ray noise data in [4]. It can be characterized as a grey box model which combines formula describing sound generation and propagation and free model input parameters. The model parameters are to be computed by means of time domain system identification from noise measurement data. The shape of the semi-empiric model ansatz function is identical to [4]:

$$(1)\quad L_i(d,\bar{\varphi},\vartheta,P_{el},\vec{p}) = 10 \cdot log_{10}\left(10^{(L_{directivity+thrust}+L_{spreading})^{1/10}} + 10^{(L_{background})^{1/10}}\right)$$

L_i corresponds to the SPL observed at observer position *i* which depends on the distance between observer and UAV d, azimuth φ and polar angle ϑ of the UAV noise emission, the UAV electric power consumption P_{el} and the model input parameter vector $\vec{p}$. The term representing thrust and directivity is reformulated in this work in (2) and (3) which enhances the independence of thrust and the directivity contribution to the overall SPL result. Additionally, term (4), which models geometric spreading, is made parameterless as the effect of atmospheric damping is removed from the noise data underlying this work.

$$(2)\quad L_{directivity+thrust}(\bar{\varphi},\vartheta,P_{el},\vec{p}) = p_1 \cdot \log(P_{el}) \cdot \frac{f_{directivity}(\bar{\varphi},\vartheta,\vec{p})}{[f_{directivity}(\bar{\varphi},\vartheta,\vec{p})]_{max}}$$

$$(3)\quad f_{directivity}(\bar{\varphi},\vartheta,\vec{p}) = \left(1 + p_2 \cdot \sin(\bar{\varphi} - p_3) \cdot \left(\vartheta + \frac{\pi}{2}\right)\left(\frac{\pi}{2}\right)\right) \cdot (1 + p_4 \cdot \sin(\vartheta - p_5))$$

$$(4)\quad L_{spreading}(d,\vec{p}) = -20 \cdot \log\left(\frac{\left|\overrightarrow{r_i^{NED}}\right|}{40\ m}\right)$$

$$(5)\quad L_{background}(\vec{p}) = p_6$$

The non-diagonal elements of the parameter error covariance matrix (PECM) indicate weather model input parameters yield linear dependencies among each other. Linear independence, which leads to a non-diagonal element entry of zero, is to be achieved in a meaningful grey box model ansatz [7, p. 377]. According to Figure 6 the PECM indicates linear dependency of parameters 1 and 5 [7, p. 111]. The situation is still acceptable as all relative standard deviations of the parameter estimates are smaller than 1 % (see Figure 7) but this indicates that the number of parameters in the current directivity function (3) should not be further increased.

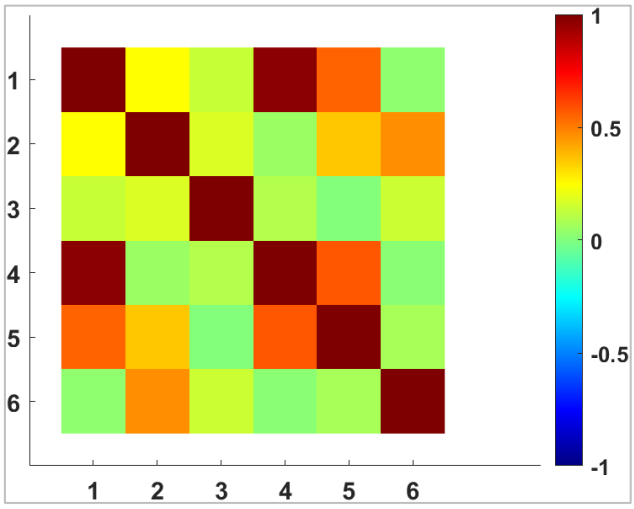

Figure 6: parameter error covariance matrix

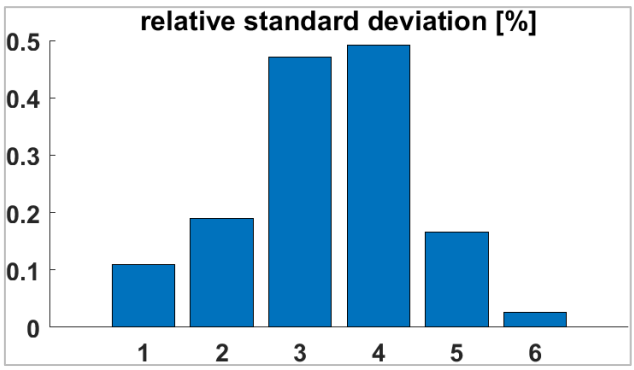

Figure 7: relative standard deviation of parameter estimates

The parameter estimates for all three model variants (all data, straight flight data only, turning flight data only) can be found in the table below. Selecting different parts of the noise data for system identification mainly affects parameters 2 to 5 which are input to the directivity function. Background noise (p_6) and the influence of P_{el} on sound generation (p_1) hardly change when selecting other parts of the noise data as input.

parameter	all data	straight flight data	turning flight data
p_1	21.851	21.428	21.666
p_2	0.230	0.243	0.182
p_3	-0.211	-0.180	-0.296
p_4	-0.283	-0.549	-0.344
p_5	1.028	0.885	1.316
p_6	39.57	39.41	39.62

Table 1: model parameters depending on modeling data source

By evaluating the semi-empiric model at constant P_{el} 'quasi' noise emission surfaces can be computed, see Figure 8. The averaged offset between surface 1 and 2 respectively between surface 2 and 3 is 0.9 dB(A) which is close to the value of the fully empiric model.

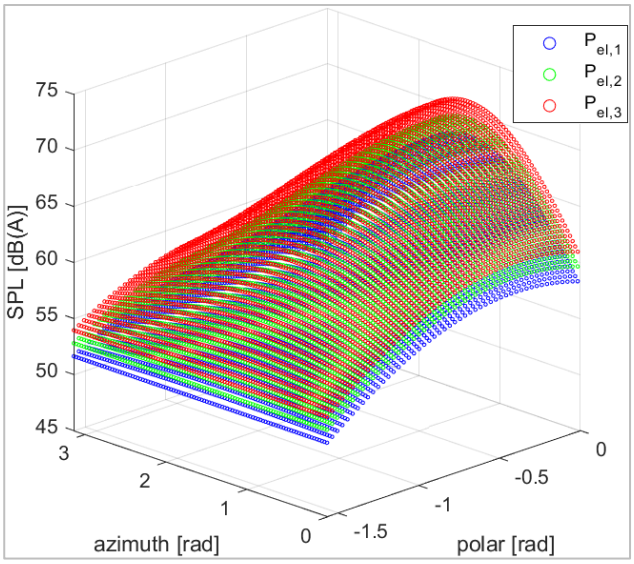

Figure 8: quasi noise emission surfaces at $P_{el,1}$=1.002, $P_{el,2}$=1.179, $P_{el,3}$=1.386;

In the case of the semi-empiric model the straight flight and the turning flight model variant do not increase the model accuracy as the 'all data' confidence bound corridor height exhibits a comparably low value at any bank angle, see Figure 9.

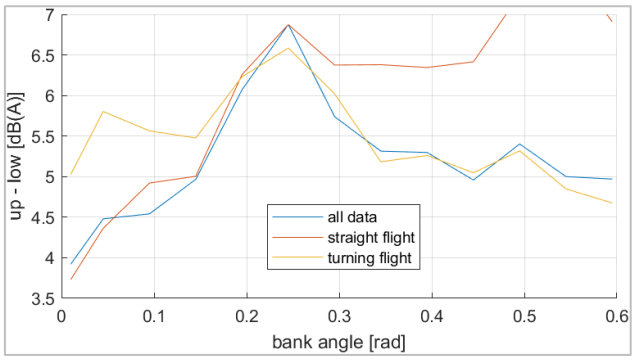

Figure 9: confidence bound corridor height for all three modelings and a confidence of 80 %; corridor height = upper bound – lower bound

3. COMPARATIVE ANALYSIS OF THE EMPIRIC NOISE MODELING APPROACHES

3.1. Comparison of Noise Emission Surfaces

A meaningful noise model comparison starts with a comparison of the noise emission surfaces, because this is where the model's noise prediction is based upon. Thus, the accuracy of the noise emission surfaces limits the overall achievable model accuracy.
Figure 10 and Figure 11 show a comparison of the (quasi) noise emission surfaces of the two noise model types deployed in this work and the respective noise measurement data points for the 'all data' and for the 'turning flight' variant. The surfaces of the fully empiric model are overall closer to the noise data. As these surfaces are not bound to a parametrization they are capable of resolving local extrema like the one at polar = -0.5 rad and azimuth = 0 rad. Nevertheless, the quasi noise emission surface of the semi-empiric model also manages to resolve the global trend of the noise data. In the case of the fully empiric modeling the standard deviation between the noise emission surfaces and the noise measurement points is 1.9 dB and in the case of the semi-empiric modeling it is 2.6 dB. The semi-empiric modeling's weaker accordance of the noise emission surfaces with the noise data confirms the observations described in this chapter.

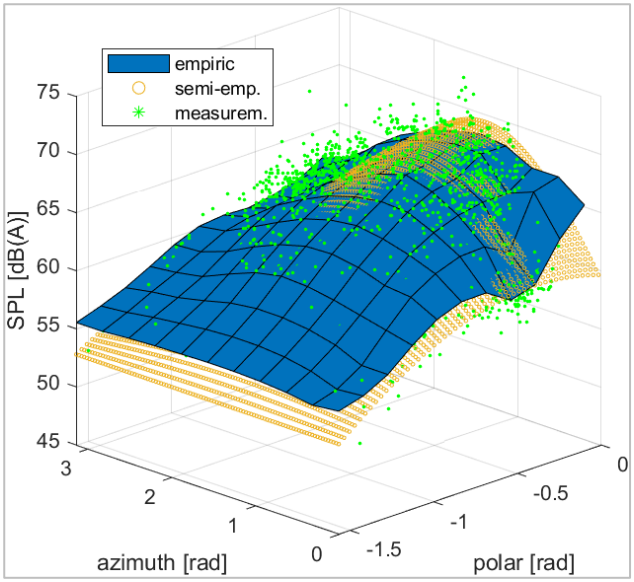

Figure 10: noise emission surface comparison with measurement data; all data; P_{el}=1.179

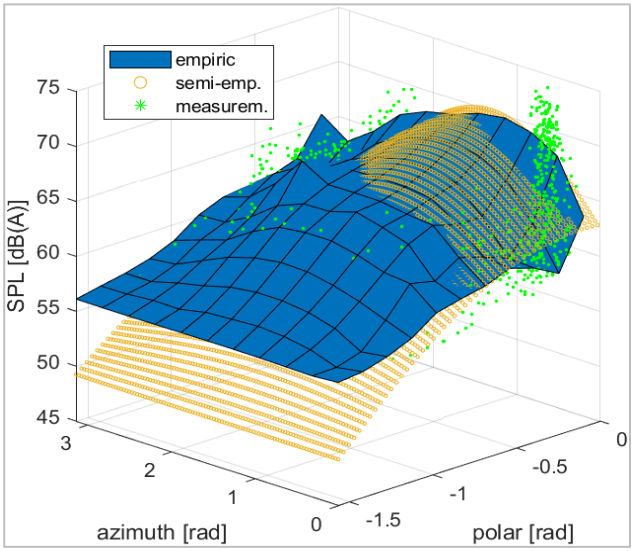

Figure 11: noise emission surface comparison with measurement data; turning flight data; P_{el}=1.354

3.2. Comparison of Mission Noise Curves

A comparison of noise model results and noise measurement data can be seen in Figure 12 and Figure 13. For both model types the following holds: During straight flights segments the confidence bounds are tightest (see e.g. flyover between t = 7160 – 7175 s) and during turning flights, where the highest SPL fluctuations occur, the confidence bounds are comparably loose (see e.g. turning flight between t = 7130 – 7155 s). This finding agrees with Figure 5 and Figure 9.

The smooth (quasi) noise emission surfaces of the semi-empiric noise model consequently lead to a SPL curve which is smoother than the one obtained from the fully empiric model. Though the fully empiric model's surfaces have more freedom to adjust to the underlying noise data this does not lead to an increase in the overall model accuracy compared to the semi-empiric model, see Table 2. Furthermore Table 2 shows that splitting the models in a turning flight model and a straight flight model does not significantly affect the model accuracy (compare lines 1 and 3 to 2 and 4).

Adding confidence bounds to the noise model prediction can be seen as a major progress compared to [4]. In case maximum allowable SPLs at observer locations exist, this feature allows a model-based prediction of the minimum allowable UAV/observer distance for a given probability.

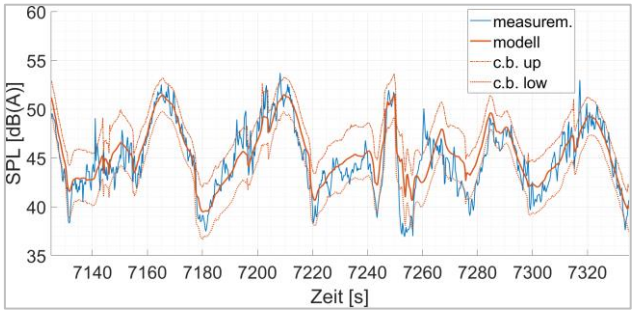

Figure 12: fully empiric model mission noise curve with 80 % confidence bounds and corresponding microphone data (mic 1)

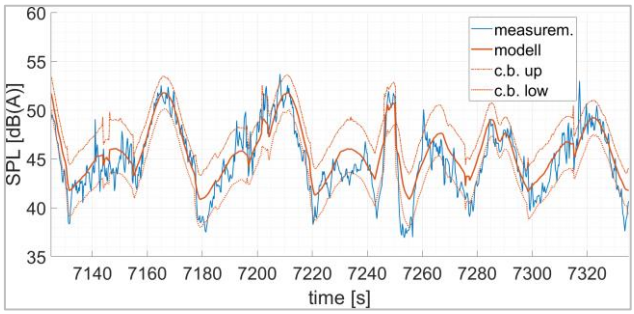

Figure 13: semi-empiric model mission noise curve with 80 % confidence bounds and corresponding microphone data (mic 1)

model (model data)	σ (all data)	σ (turning flight data)	σ (straight flight data)
semi-emp. (single model)	1.9	2.0	1.7
semi-emp. (splitted model)	1.9	2.0	1.6
fully emp. (single model)	1.9	2.2	1.6
fully emp. (splitted model)	2.0	2.2	1.6

Table 2: standard deviation σ of residual between model result and microphone data depending on model type, model variant (rows) and noise data for σ computation (columns) in dB

3.3. Comparison of Data Requirements and Modeling Effort

Though fully empiric and semi-empiric noise modeling show a similar model accuracy in the comparison compiled in this work, their data requirements are different. For a fully empiric modeling the noise measurement data must cover the whole UAV noise emission angle space that is to be modeled. This is e.g. the case in Figure 10. If no data exists for bigger parts of the noise emission angle space, the resulting noise emission surfaces will be highly dependent on the surface calculation method and therefore decrease the reliability of the resulting noise model. Semi-empiric modelings have lower noise data requirements. In case a valid model ansatz exists, which contains a priori knowledge about the UAV noise emission, full coverage of the noise emission angle space by the noise data is not mandatory. Moreover, semi-empiric modelings are of advantage in case of a low signal to noise ratio of the underlying noise data. If the model ansatz includes an estimation of the acoustic data's background noise, like it is the case in this work, then background noise is not misinterpreted as UAV noise which would lead to a noise overestimation of the noise model.
While creating a fully empiric modeling is straight forward finding a valid ansatz function for a semi-empiric modeling can be significantly more laborious. According to the author's experience it is an iterative process of defining and refining parametric ansatz functions, performing system identification computations und judging the resulting model quality.

4. DISCUSSION OF RESULTS

Possible noise model applications of the two approaches are pre-flight mission planning, flight controller integration for noise optimal onboard navigation purposes or integration into a geoinformation system for urban planning purposes.
For onboard use real-time capability is required. Evaluation of the fully empiric noise model involves several interpolation operations which can, depending on the model size and the computational capacity of the onboard hardware, lead to limitations. This, in turn, would give preference to a semi-empiric model with a compact analytical ansatz.
In case trajectory optimization and optimal navigation are targeted, continuously differentiable noise emission surfaces are of advantage as they enable efficient use of gradient-based optimization algorithms. In case of a fully empiric modeling this requirement needs to be considered in the noise emission surface computation.

5. OUTLOOK

In many cases the noise measurement data quality might be sufficient and the accuracy of the noise model predictions might be the only requirement. Under such circumstances neither fully empiric nor semi-empiric noise modeling has a dominating advantage, at least in cases where the sound generation complexity is low.
If rotorcraft or electric vertical take-off and landing vehicles (eVTOLs) are modeled, the sound generation is more complex. This added complexity is likely to give favor to semi-empiric modeling approaches which can e.g. explicitly consider effects like interference from multiple propellers.
A potential of semi-empiric noise modeling approaches is to include noise emission surface data from hybrid computational fluid dynamics (CFD)/Ffowcs Williams-Hawkings (FW-H) computations into the ansatz function definition to enhance accuracy of future modelings.

Bibliography

[1] A. Filippone und L. Bertsch, „Comparison of Aircraft Noise Models with Flyover Data," *Journal of Aircraft,* Nr. 51 (3), pp. 1043-1046, 2014.

[2] D. P. Rhodes und J. B. Ollerhead, „Aircraft Noise Model Validation," in *The 2001 International Congress and Exhibition on Noise Control Engineering*, The Hague, The Netherlands, 2001 August 27-30.

[3] M. Hornung, M. Schmähl und C. Rieger, „Zusammenfassender Abschlussbericht zum F&E Verbundvorhaben: Raumbezogene Modellierung zur Lärmreduktion elektrischer Senkrechtstarter; Vorhabensbeschreibung des Partners Lehrstuhl für Luftfahrtsysteme (TUM)," Garching, 2020.

[4] M. Schmähl, C. Rieger, S. Speck und M. Hornung, „Lärmmodellierung eines Cargo-eVTOL-UAVs mittels Systemidentifikation aus Fluglärmmessdaten in Horizontal- und Schwebeflug zum Zweck der Integration in ein Geoinformationssystem," 2020.

[5] J. D'Errico, „MATLAB Central File Exchange," 2008. [Online]. Available: John D'Errico (2021). Surface Fitting using gridfit (https://www.mathworks.com/matlabcentral/fileexchange/8998-surface-fitting-using-gridfit), MATLAB Central File Exchange. Retrieved July 29, 2021. .

[6] S. Speck, J. Wilberg und M. Hornung, „An Approach for Aeroacoustic Footprint-Modeling of Low Altitude Platforms by Means of Time Domain System Identification," in *2013 Aviation Technology, Integration, and Operations Conference*, Los Angeles, CA, 2013.

[7] R. Jategaonkar, Flight Vehicle System Identification, Reston, VA: AIAA, 2006.